Anechoic Chamber Walls: Should They be Resistive or Reactive at Low Frequencies ?

Preprint 3572 (G2-2)

D. B. (Don) Keele, Jr.
DBK Associates
Elkhart, Indiana, USA

Presented at the 94th Convention 1993 March 16–19 Berlin

AES

AN AUDIO ENGINEERING SOCIETY PREPRINT

Anechoic Chamber Walls: Should They be Resistive or Reactive at Low Frequencies?

D. B. (Don) KEELE, JR.

Audio Magazine, Hachette Magazines, Inc., New York, NY 10019, USA
Techron, Div. Crown International Inc., Elkhart, IN 46517, USA
DBK Associates, Elkhart, IN 46517, USA

This paper describes the theoretical design, and preliminary practical implementation issues, of an anechoic chamber designed specifically for spherical wave propagation. Conventional anechoic chamber design methods dictate that the acoustic impedance of the chamber's boundaries should be purely resistive (complete absorption) over the whole operational range of the chamber. For good loudspeaker measurements at low frequencies, this means large chambers and long absorptive wedges. Theory suggests that a relatively-small spherically-shaped chamber, with the source constrained to the center of the sphere, could be designed, that operates down to any arbitrary frequency, if the chamber walls are mass-reactive at lower frequencies where the wavelengths are much larger than the chamber dimensions, and absorptive at higher frequencies where the wavelengths are much shorter than the chambers dimensions.

A first-order mechanical model of the wall impedance is a massless plate, for the sound waves to impinge upon, connected to a free-standing mass through a damper. At low frequencies the whole assembly moves, thus presenting a mass reactance to the wave; while at high frequencies, the mass would be essentially immobile, and thus energy would be absorbed by the damper. The crossover point between the two modes of operation occurs at the frequency where the wavelength is equal to the circumference of the sphere, or equivalently, the radius of the sphere is about one-sixth wavelength. Derivations show that the total movable mass of the chamber's walls should be exactly equal to *three* times the mass of the air contained in the sphere. This paper explores these ideas.

0. INTRODUCTION

The main purpose of an anechoic chamber is to provide a free-field environment for acoustical testing. Traditionally, anechoic chambers are rigid-walled rectangular-shaped enclosures, with wedges of sound absorptive material, such as fiberglass, attached to the walls. The design goal for the chamber is complete absorption of all sound waves that impinge on the walls, no matter what the frequency and angle of incidence, thus achieving a reflection-free open-space-like environment. Practically, the low-frequency limit of the chamber is set by the overall dimensions of the chamber and the length of the absorptive wedges. Large chambers with long wedges are required for extended low-frequency operation.

A typical fairly-large chamber, with clear dimensions of 11.4 x 7.8 x 6.7 m (37.4 x 25.6 x 22.0 ft.) using wedges about 1.5 m (5 ft.) long, has an effective low-frequency cutoff of about 70 Hz [1. Wang], a not so very-low frequency. Operation down to say 30 Hz, would require a chamber more than twice as large in linear dimension (8 times larger in volume!), with wedges twice as long also. The 70 Hz limit assumes a source-to-sample distance which is fairly large, say on the order of 3 to 4 m, for the example chamber. Of course, the effective low-frequency limit may be extended down in frequency by decreasing the source-to-mic distance, or using nearfield measurements [2]. This unfortunately, precludes assessing the possible effects of diffraction and other source-size related effects.

A usual design requirement, for a general-purpose anechoic chamber, is the freedom to locate the acoustic source and receiver at arbitrary positions in the chamber. As a result, conventional anechoic chamber design practices dictate that the walls be as absorptive as possible at all operating frequencies and angles of incidence. This means that the walls are designed to have an absorption coefficient as close as possible to unity (1.00), and thus act as a purely-resistive (non-reactive) acoustic absorber load. Often the low-frequency cutoff of a chamber is defined at that frequency where the absorption coefficient of the absorptive wedges falls to 0.99, ie, that lower frequency where 1% of the incident energy is returned to the room [1] [3]. Another definition uses that frequency where the pressure reflection coefficient equals 0.1 or 10% [4]

Effectively, the broadband near-unity absorption coefficient of the wall treatment, implies that plane waves are assumed to hit the boundaries. This assumption fits, because it is only for progressive plane waves that the specific acoustic impedance of air, **Z**, is purely real (this impedance is the ratio of the acoustic pressure in a medium to the associated particle velocity, and is equal to $\rho_0 c$ for plane waves in air).

This is in contrast to the way that anechoic chambers are typically used, with acoustic sources that generate spherical diverging waves. For plane standing waves, or for diverging waves, **Z** is in general complex, ie, the acoustic pressure and particle velocity are not always in phase with each other [5]. This is particularly true for low frequencies, and points close to the source with respect to wavelength. This means that the chambers walls, rather than being purely resistive over the whole operating frequency range, need to have a reactive component at low frequencies. The usual justification for the design of conventional anechoic chambers, is that the walls are always many wavelengths away from the effectively spherical-wave sources, and thus experience essentially plane waves impinging on their surfaces. As will be shown, this is not true at low frequencies.

The acoustic performance of anechoic chambers is quite frequently evaluated by measuring the deviations of mean-square sound pressure, from an assumed inverse square law, as a very-small sound source and microphone are moved apart (the sound pressure should decrease by 6 dB for each doubling of distance from a point source) [1] [6]. Maximum deviations of ±0.5 dB from inverse square law, for source to microphone distances ranging over 0.5 to 6 m, are considered very good results.

This point source evaluation method, means that the most frequently used chamber evaluation technique also uses a source that generates diverging spherical waves, rather than the previously assumed plane waves. For diverging spherical waves, at distances from the source which are large compared to the wavelength (the farfield), **Z** is essentially real. In contrast, at points close to the source with respect to wavelength (the nearfield), **Z** is complex and mostly reactive, because the particle velocity has a large component out of phase with the pressure.

At frequencies below 100 Hz, the walls of most reasonably sized anechoic chambers are on the order of a wavelength or closer to the source, no matter where the source is placed. At 70 Hz in the previously mentioned chamber, a centrally mounted source is only about 1.2, 0.8, and 0.7 wavelengths from each set of walls, respectively! This means that the chambers boundary impedance needs to have a significant mass reactive component, at low frequencies, in addition to the absorptive component. Unfortunately, because of the need to locate the acoustic source at arbitrary positions in the chamber, points on the walls of a typical rectangular-shaped chamber can also be at any arbitrary distance from the source, thus making a determination of the magnitude and phase of the wall impedance nearly impossible to determine.

This paper explores the idea of a spherical- or hemispherical-shaped anechoic chamber that constrains the acoustic source to the center of the sphere (or hemisphere). This forces the walls of the chamber to be at a fixed physical distance from the source, and thus simplifies the coordination of the real and reactive parts of the wall impedance.

To eliminate wall reflections, the wall boundary mechanical impedance must match the the specific acoustic impedance of the air immediately adjacent to the boundary, both in magnitude and phase (or equivalently the real and imaginary components), at all frequencies. If this condition is met, nearly perfect inverse square law pressure variation, with distance, will occur along a radial line from the centrally-located source to the chamber's walls, at any arbitrarily low frequency! To met this boundary condition at all frequencies, it will be shown that the wall must be mass reactive and move, without absorbing, at low-frequencies, and be a rigid absorbing boundary at high frequencies.

This paper does not present a valid completely-worked-out solution to the implementation of this proposed chamber. It just presents the main ideas and some of the possible implementation problems, so that the proposal will illicit comments and discussion by others that may bring insight and possible solutions to the problems.

1. THEORY

In this section I show:

1) the equations that relate particle velocity and acoustic pressure for out-going harmonic spherical waves,

2) derive the expression for the specific acoustic impedance for this situation,

3) calculate the pressure reflection coefficient for outgoing spherical wave impinging on a perfectly-absorptive spherical boundary,

4) indicate the mechanical model for a boundary that perfectly matches the specific acoustic impedance of a out-going spherical wave (thus eliminating reflections), and

5) for the proposed spherical-shaped chamber, derive some implementation dependent relationships such as the total boundary mass required, mass per unit area of the boundary, and the required material thickness at the boundary given mass material of different densities.

1.1. Harmonic Spherical Waves

An out-going diverging harmonic spherical wave, generated by a point source or pulsating sphere, can be represented in complex form by (arrows over the variables emphasize their complex nature):

$$\vec{p} = \frac{\vec{A}}{r} e^{j(\omega t - kr)} \tag{1}$$

where

$\vec{p}$ = complex pressure

$\vec{A}$ = a complex constant

r = radial distance from center of coordinate system

ω = frequency in radians per sec ($= 2\pi f$)

f = frequency in Hz

t = time

k = wave number ($= \omega/c = \frac{2\pi}{\lambda} f$)

c = sound propagation velocity (=343 m/s = 1125 ft/s)

λ = wavelength

j = complex constant ($= \sqrt{-1}$).

The complex radial particle velocity, $\vec{u}$, is then given by [5 p. 158]

$$\vec{u} = -\frac{1}{j\omega\rho_0}\frac{\partial \vec{p}}{\partial r} = \left(\frac{1}{r} + jk\right)\frac{\vec{p}}{j\omega\rho_0} \tag{2}$$

where

ρ_0 = density of air (= 415 rayls).

Eq. (2) can be rewritten as

$$\begin{aligned}\vec{u} &= \left(\frac{1}{jr} + k\right)\frac{\vec{p}}{\omega\rho_0} \\ &= \frac{1}{\omega\rho_0}\left(k - \frac{j}{r}\right)\vec{p} \\ &= \frac{k}{\omega\rho_0}\left(1 - \frac{j}{kr}\right)\vec{p} \\ &= \frac{1}{\rho_0 c}\left(1 - \frac{j}{kr}\right)\vec{p}\end{aligned} \tag{3}$$

Eq. (3) shows the well-known fact that in the far-field, for large distances and high frequencies ($kr >> 1$), the particle velocity is in phase with the pressure. Conversely, in the nearfield at small distances and low frequencies ($kr << 1$), the particle velocity lags the pressure by 90° [5, p.158] [7, p. 346] [8, pp. 309-312].

1.2. Specific Acoustic Impedance

The specific acoustic impedance can be formed easily from Eq. (3) [9, Eq. 2.64, p. 36]

$$\vec{z} = \frac{\vec{p}}{\vec{u}} = \frac{\rho_0 c}{\left(1 - \frac{j}{kr}\right)}. \tag{4}$$

The transition between nearfield and farfield operation occurs at $kr = 1$, where the real and imaginary parts of Eq. (4) are equal, with a magnitude of $\rho_0 c/\sqrt{2}$ and phase of +45°. This relation can be rewritten in various forms as follows:

$$r = \frac{\lambda}{2\pi} \approx 0.159\lambda \approx \frac{\lambda}{6} \quad \text{and} \tag{5}$$

$$\begin{aligned} f &= \frac{c}{2\pi r} \\ &\approx \frac{54.6}{r_{\text{in meters}}} \\ &\approx \frac{179}{r_{\text{in feet}}} \end{aligned} \quad . \tag{6}$$

Eq. (5) shows that the transition region occurs at the point whose distance is about one-sixth wavelength from the source. Eqs. (6) indicate, for example, that for a point that is about 2 m from a point source, the transition occurs at about 27 Hz.

Note in passing, that the form of Eq. (4) is exactly the same as the steady-state sinusoidal electrical input impedance of a resistor in parallel with an inductor (parallel LR circuit), or the reciprocal of the input impedance of resistor in series with a capacitor (a series RC circuit, the dual of the parallel LR circuit).

1.3. Pressure Reflection Coefficient

To evaluate the effectiveness of a chambers boundary, the complex pressure reflection coefficient can be evaluated. This coefficient is given as follows, where it is borrowed from transmission line theory [10, pp. 19 and 26] [11, where it was applied to the mismatch that occurs at the mouth of a horn]. Note that a reflection coefficient of zero is the desired goal. Any non-zero value indicates pressure reflections.

$$\vec{K}_P = \frac{\vec{Z}_L - \vec{Z}_0}{\vec{Z}_L + \vec{Z}_0} \quad . \tag{7}$$

where

$\vec{K}_P$ = complex pressure reflection coefficient

$\vec{Z}_L$ = complex acoustic load impedance

$\vec{Z}_0$ = complex acoustic impedance of transmission media.

If a spherical-shaped anechoic chamber, of radius R, with a centrally located acoustic source is assumed (Fig. 1), all boundary points on the chambers walls are equal (or approximately equal) distances from the source. The reflection coefficient can be evaluated for this situation, and indicates how well the boundary minimizes reflections.

The reflection coefficient can be evaluated for a perfectly absorptive boundary, by using a load impedance equal to $\rho_0 c$ at all frequencies ($\vec{Z}_L = \rho_0 c$, purely real!), and the impedance of the transmission media equal to the specific acoustic impedance of outgoing spherical waves, given by Eq. 4, with the radius equal to the radius of the chamber, R. This situation mirrors the target conditions for a conventional anechoic chamber where the goal is to completely absorb incident plane waves, but evaluates the reflections for incident spherical waves. The reflection coefficient for this situation is derived as follows:

$$\vec{K}_P = \frac{\vec{Z}_L - \vec{Z}_0}{\vec{Z}_L + \vec{Z}_0} = \frac{\rho_0 c - \dfrac{\rho_0 c}{\left(1 - \dfrac{j}{kR}\right)}}{\rho_0 c + \dfrac{\rho_0 c}{\left(1 - \dfrac{j}{kR}\right)}}$$

$$= \frac{1 - \dfrac{1}{\left(1 - \dfrac{j}{kR}\right)}}{1 + \dfrac{1}{\left(1 - \dfrac{j}{kR}\right)}}$$

$$= \frac{-\dfrac{j}{kR}}{\left(2 - \dfrac{j}{kR}\right)} = \frac{-j}{2kR - j}$$

$$= \frac{1}{1 + j2kR} \tag{8}$$

The absolute value of this expression may be taken

$$\left|\vec{K}_P\right| = \frac{1}{\sqrt{1 + 4(kR)^2}} \tag{9}$$

For small kR ($kR << 1$), this function is essentially equal to one ($|\vec{K}_P| = \vec{K}_P = 1$), which means that all the pressure waves are reflected back to the source, just as if the wall were rigid and non absorbing! For large kR ($kR >> 1$), this function approaches zero and decreases inversely with kR ($|\vec{K}_P| \approx \frac{1}{2kR}$), and means that out-going energy is mostly absorbed, rather than being reflected.

Figs. 2 and 3 show plots of the absolute value of the reflection coefficient for the case of a spherical chamber whose boundary is perfectly absorptive at all frequencies, Eq. (9), plotted on linear and log scales respectively. Note that to absorb 90% of the energy or reflect back 10 % ($|\vec{K}_P| = 0.1$), a kr of about 5 is required. This means that the walls must be beyond about 0.8 wavelengths from the source at the lowest frequency. A more stringent condition would be to absorb 99% of the energy and reflect only 1% ($|\vec{K}_P| = 0.01$). A very large kr of 50 is required for this situation. This would require the walls to be about 10 times farther from the source (about 8 wavelengths), for the same low-frequency limit! Clearly a pure $\rho_0 c$ boundary for the spherical anechoic chamber is undesirable!

1.4. Boundary Mechanical Model to Match Air Impedance

The reflection coefficient may be minimized at all frequencies, by matching the boundary mechanical impedance to the specific acoustic impedance of the outgoing spherical waves at the chambers walls. This requires that the both the real and imaginary parts of the specific acoustic impedance, considered separately, be matched at all frequencies. The specific acoustic impedance at the chambers walls is given by Eq. (4), with the radius equal to the radius of the spherical chamber, R. It is noted in passing that the required boundary impedance is identical to the radiation impedance of a spherical source whose radius is equal to the radius of the chamber. For the mechanical impedance of the wall to equal this value, the equivalent mechanical model for the load must be determined.

1.4.1. Configuration of Mechanical Model

As Beranek shows, the equivalent analogous electrical circuit to the specific acoustic impedance of Eq. (4) is an inductor in parallel with a resistor, shown in Fig. 4. [9, pp. 47-55, and pp. 144-125]. This circuit follows his "Impedance" analogy, where the voltage and pressure, and the current and particle velocity are analogous quantities.

As Beranek also shows, the analogous mechanical model is a damper (which provides mechanical resistance) hooked to a free standing mass. This is shown in Fig. 5. This model follows Beranek's Impedance analogy, where the voltage and force, and the current and velocity are analogous quantities.

In this situation, the force is applied to the damper, which in turn moves the mass. This model intuitively fits the impedance function of Eq. (4), because at high-frequencies the force required to move the mass far exceeds the force required to expand and compress the damper, thus the mass stays essentially stationary, and all the power is absorbed by the damper, forming a real load. At low frequencies, the force required to expand and compress the damper greatly exceeds the force required to move the mass, thus the damper and mass move together and form a reactive mass load.

One more item needs to be added to the model; a means for converting the acoustic pressure of the sound wave into a force that in turn moves the mechanical assembly. This is a massless plate, of area A, attached to the damper for the acoustic waves to impinge upon. This revised model is shown in Fig. 6. Please realize that this is only a mechanical model for the wall termination. The actual details of a specific implementation may be quite different.

1.4.2. Calculation of Mass

The only remaining item to calculate, is the required value of mass to properly match the airs reactive component. This may be calculated by using Newtons law of motion that relates the force applied to a mass and its resultant acceleration, but for periodic sinusoidal motion:

$$F_T = m_T\, a = m_T \frac{du}{dt} = j\omega m_T\, u \tag{10}$$

where

m_T = total mechanical mass of spherical boundary
a = acceleration of boundary
u = velocity of boundary
F_T = total force applied to boundary.

This equation can in turn be solved for mass yielding

$$m_T = \frac{F_T}{j\omega u} = -\frac{jF_T}{\omega u} \tag{11}$$

For acoustical systems the force is equal to the the pressure times the area

$$F_T = pS_T \tag{12}$$

where

p = pressure
S_T = area of boundary.

Substituting Eq. (12) into Eq. (11) yields

$$m_T = -\frac{p}{u} \cdot \frac{S_T}{\omega} j \tag{13}$$

For low frequencies and points close to the source with respect to wavelength, the specific acoustic impedance Eq. (4), evaluated at the boundary radius R, simplifies to

$$\vec{z} = \frac{\vec{p}}{\vec{u}} = \frac{\rho_0 c}{\left(1 - \frac{j}{kR}\right)} \approx \frac{\rho_0 c}{-\frac{j}{kR}} = j\rho_0 ckR = j\omega\rho_0 R \tag{14}$$

When this expression for p/u is substituted into Eq. (13), and knowing that the area of the sphere is $S_T = 4\pi R^2$, the following results

$$m_T = 4\pi R^3 \rho_0 . \tag{15}$$

This can be slightly rewritten in the form of .

$$m_T = 3\left(\frac{4}{3}\pi R^3 \rho_0\right). \tag{16}$$

The quantity in brackets is recognized as being the mass of air contained within the spherical chamber. Therefore the the required boundary mechanical mass is exactly *three* times the mass of the air contained in the chamber! This last relationship is also pointed out by Skudrzyk in a derivation based on the kinetic energy of the mass [7, pp. 350 and 353].

The mass per unit area (mass area density), of the spherical boundary, may be calculated by dividing Eq. (15) by the area of the sphere ($S_T = 4\pi R^2$) yielding

$$m_S = \frac{m_T}{S_T} = R\rho_0 . \tag{17}$$

This relationship shows that the mass area density rises in direct proportion to the radius of the spherical boundary.

Given a specific material to form the boundary mass, the required thickness of the material may be derived dividing the mass per unit area of the boundary, by the density, ρ_M, of the material used to form the mass:

$$T = \frac{m_S}{\rho_M} = \frac{\rho_0}{\rho_M} R . \tag{18}$$

This shows that the required thickness varies as the ratio of the density of air to the density of the material, and increases in direct proportion to the boundary radius.

1.5. Implementation Issues

Considering only factors in implementing the moving mass, Table 1 shows various parameters calculated for a range of chamber sizes spanning a radius range of 1 to 25 m in third octave steps. These parameters include: sphere radius, sphere surface area, sphere volume, air mass inside sphere, boundary moving mass, boundary moving mass per unit area, and the required thickness for four representative materials used to form the mass, including glass wool (50 kg/m^3, approximate density of glass wool used to form wedges in a chamber), water (1,000 kg/m^3), aluminum (2,700 kg/m^3), and lead (11,300 kg/m^3).

Somewhat surprising, are the small values of material thickness required for the moving mass at the boundary. For example, a reasonable-sized spherical chamber of 3.15 m radius, requires mass thicknesses of 76.2, 3.8, 1.4, and 0.34 mm, respectively for the four materials (glass wool, water, aluminum, and lead).

Figure 7 shows a cross section of a chamber which utilizes the mechanical wall termination model of Fig. 6 to form the boundary. In this depiction, the boundary has been divided up into 20 small mass-damper combinations. Obviously, this type of direct implementation is not very practical.

A more practical implementation of the wall termination might consist of many freely suspended chunks of fiberglass wool, that move without absorbing at low-frequencies, and absorb without moving at high frequencies. A anechoic chamber, informally called an "Acoustic Jungle" by its designer, constructed by Bruel and Kjaer, uses a technique similar to this (actually, B&K has constructed several of these chambers in Denmark). The chamber, based on a technique proposed by Dr. Eng. L. Cremer of the Technical University of Berlin, Germany, in the early sixties, was made for reasons of ease of construction, low cost, and superior high-frequency absorption [12] [13]. Apparently, it was not designed to deliberately match the acoustic impedance of spherical waves, by being mass reactive at low frequencies and absorptive at high frequencies.

This chamber construction method lines the walls of the room with freely suspended cubes of glass wool of different sizes and densities, with the larger cubes closest to the wall and the smaller ones farther out. The cubes are attached to wires or strings freely hung from the ceiling. A rough depiction of this method, but showing only two sizes of cubes, is shown in Fig. 8. In practice, the cubes are hung in random positions and orientations, which is not shown in the figure. The basic idea of the lining is that from an acoustical point of view, it represents a large irregular surface which absorbs sound from many directions. Fig. 9 shows one of the B&K chambers designed and constructed using these methods.

To the best of my knowledge, only two chambers in the United states have been constructed using the hanging wads of glass wool technique: one at the R & D facilities of Harman-Motive Inc., a loudspeaker manufacturer, installed by John King (now retired) [14], and the other at company that prefers to stay anonomous [15]. Chambers using this construction technique are said to have improved low-frequency performance as compared to conventional chambers using the wedge-attached-to-the-wall technique [16] (I was unable to find any hard evidence for this claim, however. Refs 12 and 13 did not mention this.).

2. ACOUSTIC-FIELD SIMULATIONS

The original impetus for this paper started back in January 1978, when I was doing simulations using a two-dimensional acoustic wave simulation program that I had developed, that used electric network finite elements [16]. I had used the program to predict the steady-state sinusoidal pressure magnitude and phase in a number of well known situations, where I thought I knew what the answers would be. These situations included, among others, a straight duct, a Helmholtz resonator, an expansion chamber muffler, and standing waves in a reverberation chamber.

Every simulation went as I expected until I got to the one where I attempted to simulate an anechoic chamber, by analyzing wave propagation for a constant-pressure point source in a 90° corner, with a pure resistive absorptive termination at its output. I fully expected decreasing sound pressure the farther a point was from the source, at all frequencies. At mid and high frequencies, everything went as expected. However, as frequency was lowered, the sound pressure distribution approached that of a sealed chamber, ie the pressure was everywhere the same and equal to the source, and did not decrease with distance from the source! After much thought, and reference to my college acoustics texts, I finally figured out what was happening. The purely real termination was not a proper match to the impedance of the expanding wave, which I should have known all the time!

Figs. 10, 11, and 12 show the results of these original simulations run in 1978. The original simulations were done using a time-shared computer system, in batch mode, with all output printed on a Teletype in text. Here, I have created pressure contour plots from the original data, using the math program Mathematica (this program was also used for the 3D depictions in Figs. 1 and 8). In each plot, the constant pressure source is in the lower left corner of the square region. The simulations used 13 square finite elements, each with four nodes (a total of 22 nodes with connections), in a basic 4 x 4 array, with the three elements farthest from the source removed, Fig. 10. This formed an approximate circular boundary at a constant distance from the source. The left and bottom walls (nodes) were unterminated, which represents a rigid boundary. The top and right boundaries, were all terminated in a pure resistance, or a complex load. The program calculated the pressure magnitude and phase at each node.

The simulation results for these two boundary conditions are shown in Figs. 11 and 12. Frequency was varied so that the distance represented on the side of the 4 x 4 element square was 0.5, 0.05, and 0.005 wavelength respectively, going from high to low frequency (top to bottom in the figures).

Figure 11 shows the pressure distribution results for the situation of a pure real load that matches the characteristic impedance of the model. Note that at the highest frequency, the pressure drops as you get farther from the source, as expected. However, as frequency is lowered, the pressure distribution rather than rolling off with distance from the source, approaches a constant at all points equal to the level of the source!

Figure 12 shows the results with the proper complex termination, that goes mass reactive at low frequencies (this was a parallel LR circuit in the model). The pressure distributions roll off with distance from the source, at all frequencies, as expected.

The distribution anomalies in the center of the top plot are due to errors generated by the model, because the simulation is at the highest frequency where the model gives fairly accurate results. Eight elements per wavelength are required at the highest frequency. In these plots, the node values for the missing elements, that are farthest from the pressure source, were extrapolated so that the data set formed a square region for plotting purposes.

3. CONCLUSIONS

The answer to the question posed in the title of this paper: Anechoic Chamber Walls: Should They be Resistive or Reactive at Low Frequencies? is yes! Even though conventional chambers are designed to completely absorb plane waves at any angle of incidence, and at any frequency in their bandwidth of operation, plane waves seldom impinge on the walls. Most typical sources used in anechoic chambers generate spherical waves rather than plane waves. At low frequencies, where a boundary is a small fraction of a wavelength away from the source, the boundary impedance needs to have a significant mass reactive component in order to match the acoustic impedance of the impinging spherical wave. This minimizes reflections.

Unfortunately, for a conventional rectangular chamber, where the source and receiver can be at arbitrary locations, it is impossible to coordinate the desired complex boundary impedance because the walls can be any arbitrary distance from the acoustic source. Conventional chamber design practices, which dictate that the wall impedance be purely real and absorptive over the whole operating range of the chamber, seem to work well in this situation.

This paper proposes a spherical or hemi-spherical shaped chamber, with source in the center, that places the chambers walls at a constant distance from the source, and thus can be properly coordinated for a complex wall impedance that matches the outgoing spherical waves.

It was shown that the mechanical model of the proper wall termination is a massless plate, for the waves to impinge upon, attached to a viscous damper connected to a freely suspended mass. At high frequencies, where the walls are in the farfield of the source, most of the incident energy is absorbed in the damper because the mass essentially does not move. At low frequencies, where the chamber's walls are in the nearfield of the source, the whole assembly moves and therefor presents a non-absorptive mass-reactive impedance to the wave. This termination properly matches the wall impedance to the acoustic impedance of the diverging spherical waves, thus minimizing reflections at all frequencies. Theoretically the chamber should operate down to any arbitrarily low frequency, assuming the mass-damper assemblies can oscillate over a large enough amplitude.

Several parameters for the moving-mass termination model were derived, including total mass required (which ended up being equal to three times the mass of the air contained in the sphere), mass per unit area, and the required thickness of material to form the mass. A table giving these parameters for a range of chamber radii was presented, along with the required thickness of several different types of material.

An existing chamber construction method, that uses hunks of different sized glass wool freely suspended by string or wire from the chamber's ceiling, was shown to be a possible solution to the implementation of the boundary model. At high frequencies, the hunks of glass wool are mostly stationary and thus are good absorbers. At low frequencies, the glass wool hunks move with the incoming wave pressure variations, and thus present a mass reactance with low absorption.

Unfortunately, a practical implementation of the scheme has not yet been determined. Suggestions, observations, and ideas to produce a workable implementation, are welcome,

4. ACKNOWLEDGEMENT

I would like to acknowledge the assistance and comments of several people including: Steve Temme and Gunner Rasmussen of B&K Denmark who supplied references [12] , [13], and the photo of Fig. 9, Douglas O'Brien and John King of Harman-Motive for leads on the source of their chamber; and to Prof. Jiri Tichy. of Pennsylvania State University, Earl Geddes of Ford Motor Company, and to Prof. William Strong of Brigham Young University, for their comments and discussions. Thanks also go to Tom Lininger of Crown International for references [3] and [4], and for some of the history behind the anechoic chamber installed at Electro-Voice in the late 60's.

5. REFERENCES

[1] J. Wang and B. Cai, "Calculation of Free-Field Deviation in an Anechoic Chamber," *J. Acoust. Soc. Am.*, vol. 85(3), pp. 1206-1202 (1989 Mar.).

[2] D. B. Keele, Jr., "Low-Frequency Loudspeaker Assessment by Nearfield Sound-Pressure Measurement," *J. Audio Eng. Soc.*, vol. 22, pp. 154 - 162 (1974 Apr.).

[3] Industrial Acoustics Company, "Anechoic Rooms," Bulletin AN-33R1, (Bronx, NY, USA, 1962).

[4] Eckel Corporation, "Anechoic Chambers," Engineering sales document, (Cambridge, MA, USA, 1956).

[5] L. E. Kinsler and A. R. Frey, *Fundamentals of Acoustics* (Wiley, New York, 1962).

[6] W. Koidan and G. R. Hruska, "Acoustical Properties of the National Bureau of Standards Anechoic Chamber, " *J. Acoust. Soc. Am.*, vol. 64(2), pp. 508-516 (1978 Aug.).

[7] E. Skudrzyk, *The Foundations of Acoustics* (Springer-Verlag, New York, 1971).

[8] P. M. Morse and K. U. Ingard, *Theoretical Acoustics* (Princeton University Press, New Jersey, 1968).

[9] L. L. Beranek, *Acoustics* (American Institute of Physics, New York, 1986).

[10] R. G. Brown, R. A. Sharpe, and W. L. Hughes, *Lines Waves and Antennas* (The Ronald Press Company, New York 1961).

[11] D. B. Keele, Jr., "Optimum Horn Mouth Size," presented at the 46th Convention of the Audio Engineering Society, (1973 Sept.), preprint 933 (B-7).

[12] G. Rasmussen, "Anechoic Sound Chambers," Bruel & Kjaer design document (1972 Sept.).

[13] C. Fog, "Anechoic Chamber at Bruel & Kjaer," *Proceedings of the Nordic Acoustical Meeting* at Aelborg, Denmark, pp. 285-288 (1986 Aug.).

[14] D. O'Brien, Manager of Engineering, Harman-Motive Inc., 1201 South Ohio St., Martinsville, IN 46151, Phone: (317) 342-5551.

[15] Anonomous source.

[16] Private communications

[17] D. B. Keele, Jr., "AWASP: An Acoustic Wave Analysis and Simulation Program," presented at the 60th Convention of the Audio Engineering Society, (1978 May), preprint 1365 (D-8).

TABLE 1., CHAMBER MASS PARAMETERS									
SPHERE RADIUS	SPHERE SURFACE AREA	SPHERE VOLUME	AIR MASS INSIDE SPHERE	BOUNDARY MOVING MASS	BOUNDARY MASS per UNIT AREA	MATERIAL THICKNESS WOOL	WATER	ALUM.	LEAD
m	sq. m	cu. m	kg.	kg.	kg./cu. m	mm	mm	mm	mm
1	12.6	4.2	5.1	15.2	1.21	24.20	1.21	0.45	0.11
1.25	19.6	8.2	9.9	29.7	1.51	30.25	1.51	0.56	0.13
1.6	32.2	17.2	20.8	62.3	1.94	38.72	1.94	0.72	0.17
2	50.3	33.5	40.5	121.6	2.42	48.40	2.42	0.90	0.21
2.5	78.5	65.4	79.2	237.6	3.02	60.50	3.03	1.12	0.27
3.15	124.7	130.9	158.4	475.3	3.81	76.23	3.81	1.41	0.34
4	201.1	268.1	324.4	973.1	4.84	96.80	4.84	1.79	0.43
5	314.2	523.6	633.6	1900.7	6.05	121.00	6.05	2.24	0.54
6.3	498.8	1047.4	1267.3	3802.0	7.62	152.46	7.62	2.82	0.67
8	804.2	2144.7	2595.0	7785.1	9.68	193.60	9.68	3.59	0.86
10	1256.6	4188.8	5068.4	15205.3	12.10	242.00	12.10	4.48	1.07
12.5	1963.5	8181.2	9899.3	29697.9	15.12	302.50	15.13	5.60	1.34
16	3217.0	17157.3	20760.3	62280.9	19.36	387.20	19.36	7.17	1.71
20	5026.5	33510.3	40547.5	121642.5	24.20	484.00	24.20	8.96	2.14
25	7854.0	65449.8	79194.3	237582.9	30.25	605.00	30.25	11.20	2.68

Table 1. Various parameters for the optimum boundary termination for a spherical anechoic chamber, are calculated for a range of chamber sizes spanning a radius range of 1 to 25 m in third octave steps. These parameters include: sphere radius, sphere surface area, sphere volume, air mass inside sphere, boundary moving mass, boundary moving mass per unit area, and the required thickness for four representative materials used to form the mass, including glass wool (50 kg/m^3, approximate density of glass wool used to form wedges in a chamber), water (1,000 kg/m^3), aluminum (2,700 kg/m^3), and lead (11,300 kg/m^3).

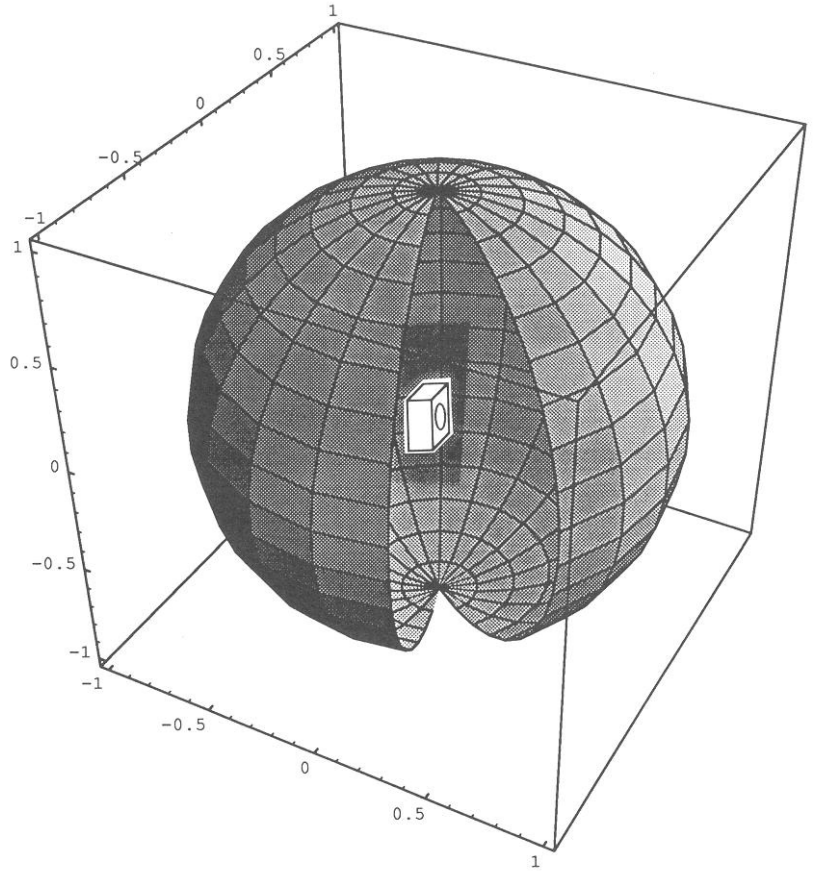

Fig. 1. Depiction of a spherical-shaped anechoic chamber, with the sound source mounted in center. This style chamber places all the chamber's boundary surfaces at a constant distance from the source. This allows coordination of the boundary's mechanical impedance to properly match the acoustic impedance of the outgoing spherical waves, thus eliminating reflections. The boundary's walls should move without absorbing at low frequencies (where the walls are close to the source with respect to wavelength), and absorb without moving at high frequencies (where the walls are far from the source with respect to wavelength). This theoretically allows perfect inverse-square roll off of pressure down to any arbitrary low frequency.

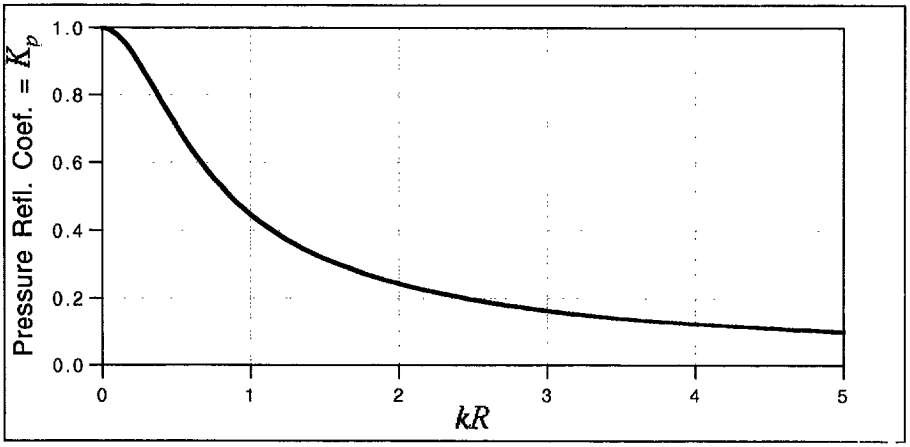

Fig. 2. Plot of the absolute value of the pressure reflection coefficient as a function of kR, Eq. (9), for the situation of a completely-absorptive resistive boundary, at all frequencies, on the inside surface of the spherical anechoic chamber shown in Fig. 1, plotted on linear scales. Note that at low-frequencies, where the boundary is close to the source with respect to wavelength ($kR << 1$), the pressure waves are completely reflected from the boundary. At high frequencies, where the boundary is far from the source with respect to wavelength ($kR >> 1$), most sound is absorbed. The reflections at low frequencies are due to the mismatch between the out-going spherical wave's acoustic impedance, and the terminating mechanical impedance of the walls.

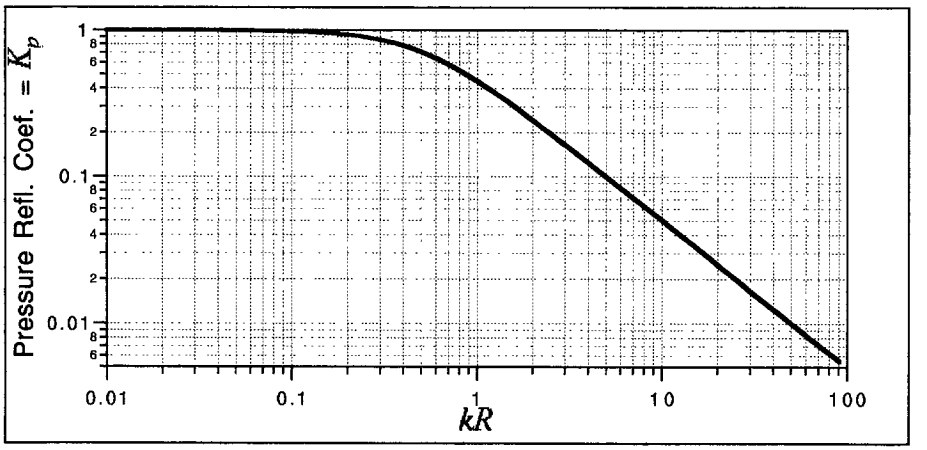

Fig. 3. Plot of the pressure reflection coefficient data of Fig. 2, but plotted on log-log scales. See Fig. 2 caption.

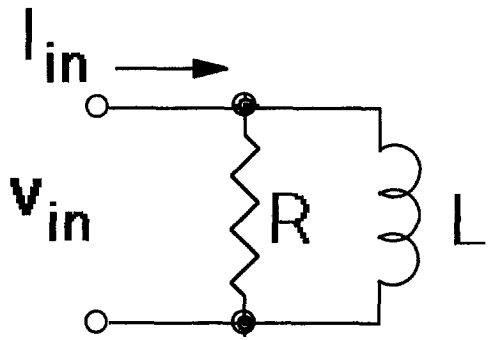

Fig. 4. Equivalent analogous electrical circuit for the specific acoustic impedance function of Eq. (4). This parallel inductor-resistor equivalent circuit has the same form of electrical input impedance as the acoustic impedance of an outgoing spherical wave. In this circuit model, the electrical voltage and acoustical pressure, and the current and particle velocity are analogous quantities. Note that at high frequencies ($\omega >> L/R$ analogous to $kr >> 1$) the circuit is resistive, and for low frequencies ($\omega << L/R$ analogous to $kr << 1$) the circuit's impedance is very low and reactive.

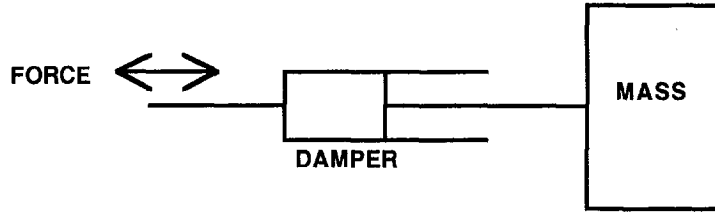

Fig. 5. Equivalent analogous mechanical model for the specific acoustic impedance function of Eq. (4) or the electric network of Fig. 4. The model is a force applied to a viscous damper, which provides mechanical resistance, which in turn is hooked to a free standing mass. At high frequencies, the mass, due to inertia, is unmoving and all the energy is absorbed in the damper. At low frequencies, the force required to compress and expand the damper far exceeds the force required to move the mass, thus the whole assembly moves without absorbing, and presents a low reactive mechanical impedance (force divided by velocity) to the source.

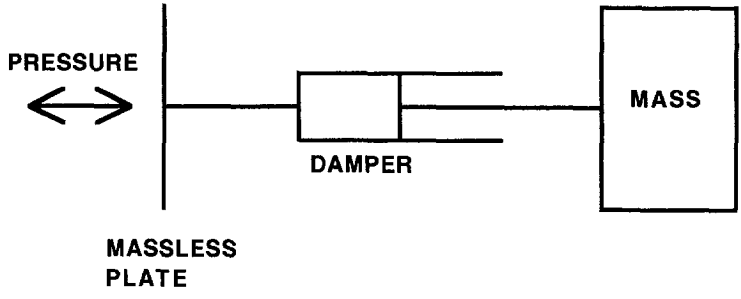

Fig. 6 Equivalent analogous mechanical model for the specific acoustic impedance function of Eq. (4), but with a massless plate added so that the pressure of the impinging acoustical waves will translate to a force on the damper. This is the mechanical model of the proper boundary termination for the spherical anechoic chamber of Fig. 1, that properly matches the acoustic impedance of the outgoing spherical waves.

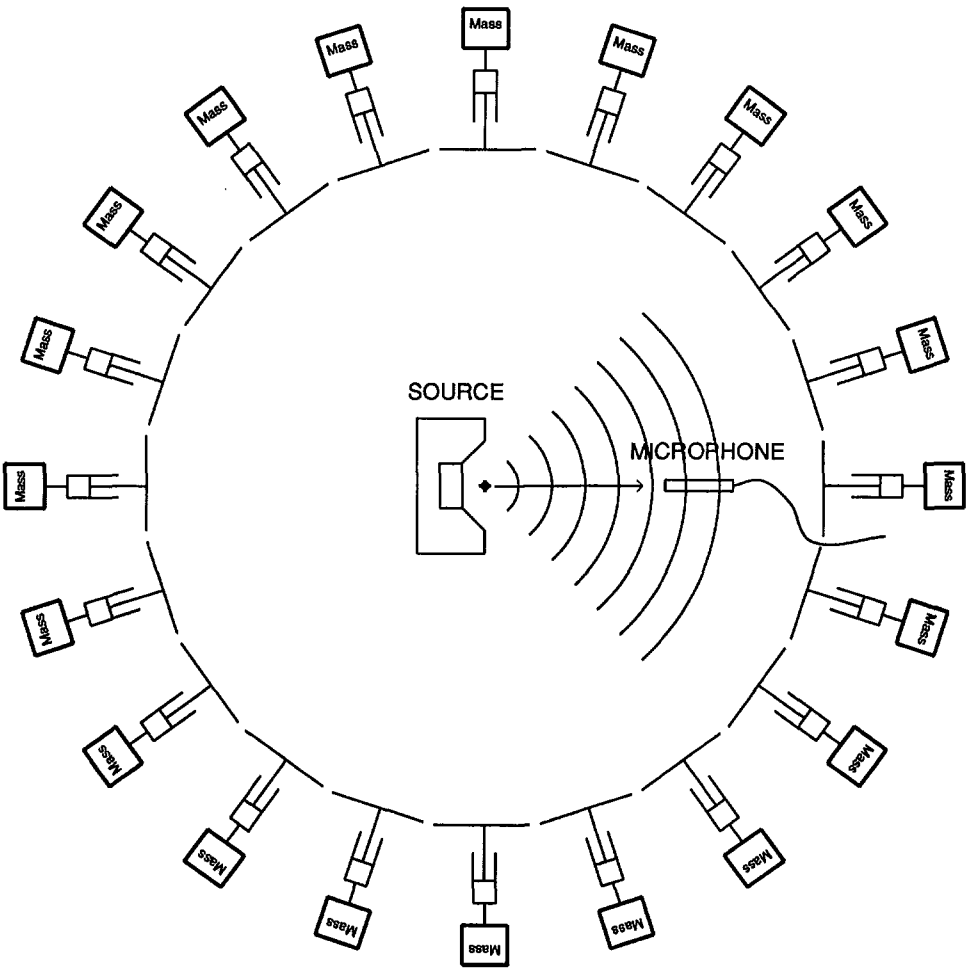

Fig. 7 Cross section of the spherical anechoic chamber of Fig. 1, showing how 20 small mechanical mass-damper models of Fig. 6 might be used to form the correct wall termination mechanical impedance.

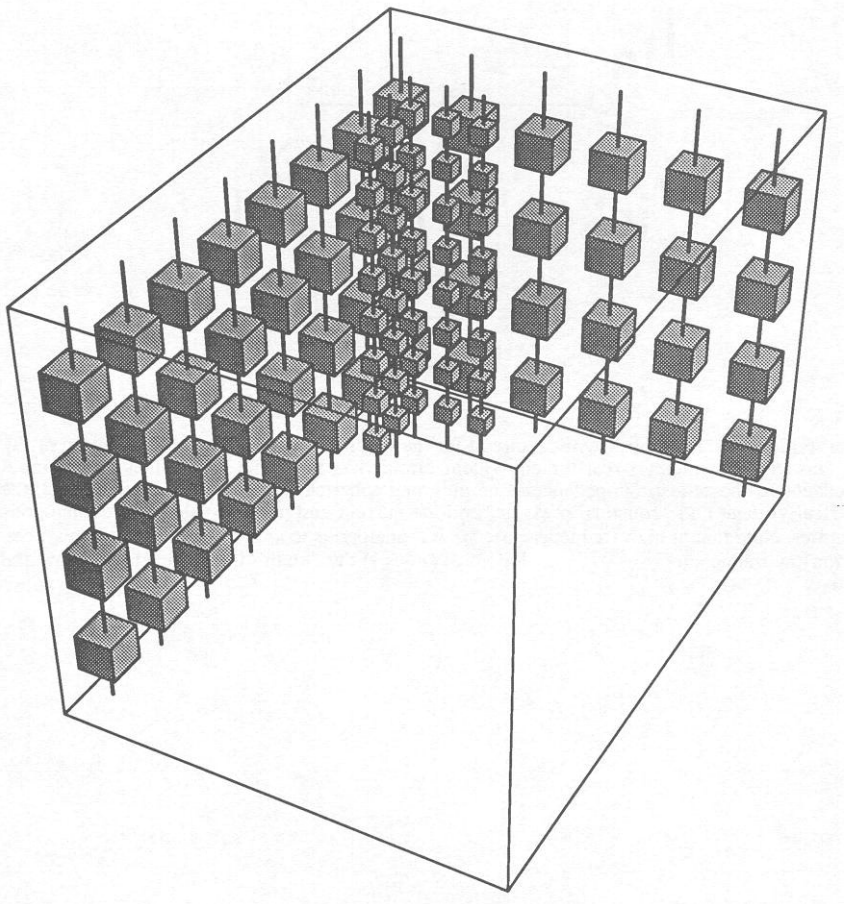

Fig. 8 Depiction of an idealized rectangular anechoic chamber that uses freely hanging cubes of glass wool to absorb sound, called an "Acoustic Jungle." In practice, many more cubes would be used, of differing sizes and wool density, placed at random locations and orientations. The larger cubes would be hung closer to the wall. Although this lining method was not specifically designed to absorb low frequencies by moving rather than absorbing, as suggested in this paper, it may work better at low frequencies as well.

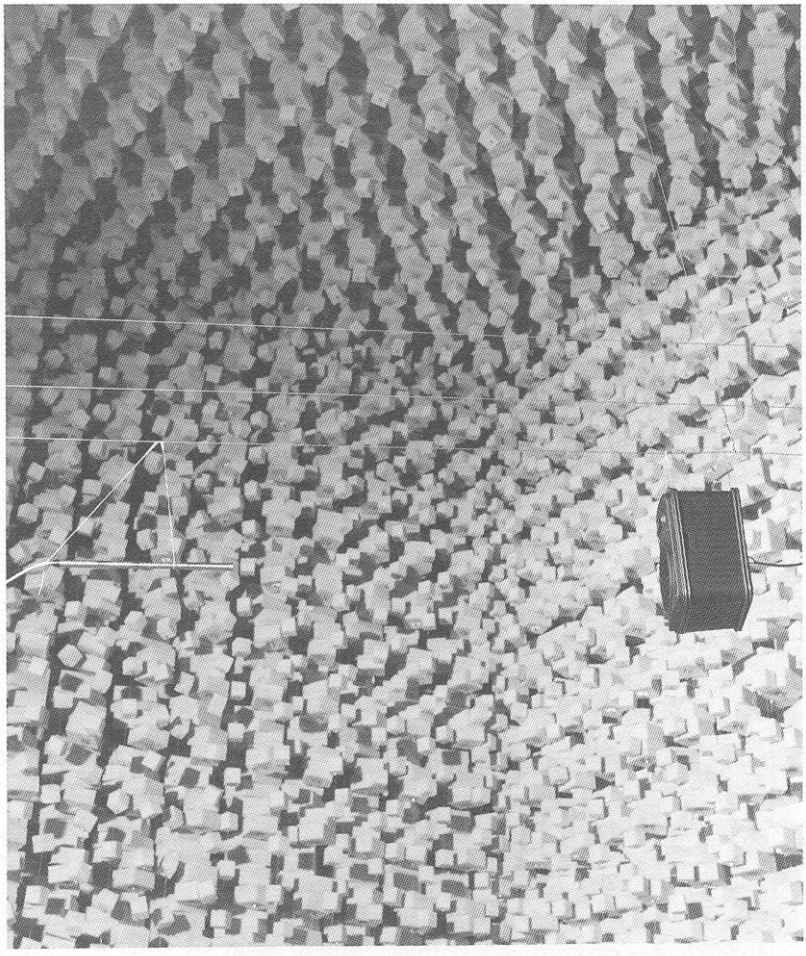

Fig. 9 A practical application of Fig. 8, an anechoic chamber using the "Acoustic Jungle" method of freely-hanging wads of glass wool to absorb sound (courtesy of Bruel & Kjaer).

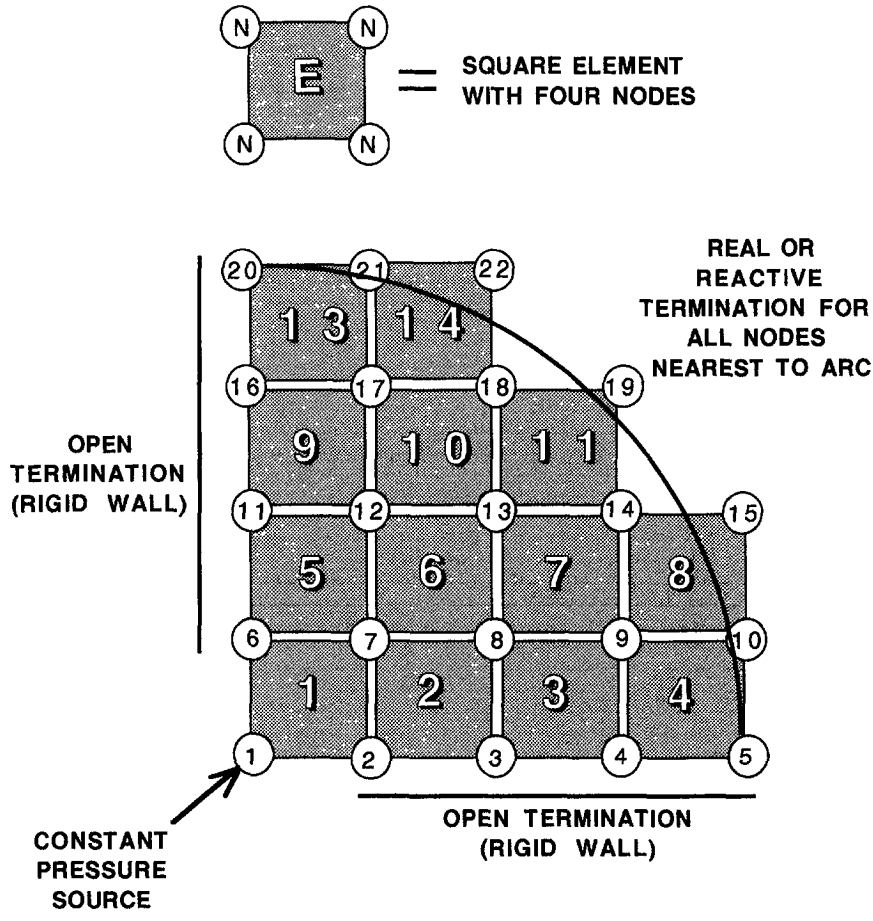

Fig. 10 Depiction of a 2D finite-element model used to simulate free-space propagation of sound in a 90° corner, with anechoic terminations on the other end. A constant-pressure sound source is located at the apex of the rigid side walls at the lower left of the diagram. An absorptive (resistive) or complex absorptive/reactive termination is applied to the nodes along the boundary farthest from the source (nodes closest to the circle). In this model, the theoretical wavefronts are circles diverging from the corner source. A proper boundary termination will absorb outgoing waves and thus exhibit inverse rolloff of pressure the farther from the source. The model is composed of 14 side-by-side square elements, with 22 nodes where the sound pressure is calculated.

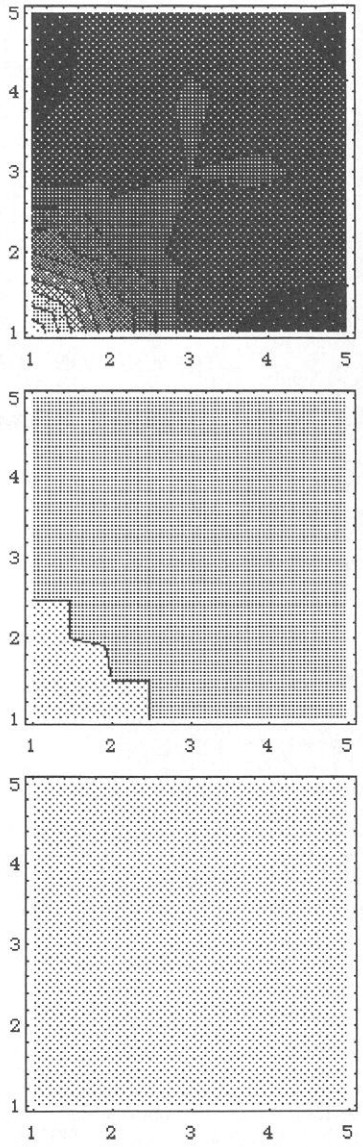

Fig. 11, Pressure contour distribution plots for the model of Fig. 10, for a pure real termination along the outside boundary. (a) Mid frequency where the side walls are 0.5 wavelength long. (b) Low frequency where the sidewalls are 0.05 wavelength long. (c) Very low frequency where the sidewalls are 0.005 wavelength long. There is approximately 12 dB variation between lightest and darkest areas of the plots. Note that as the frequency is lowered, the pressure distribution reaches a constant equal-to-the-source level at all points, rather than decreasing the farther from the source!

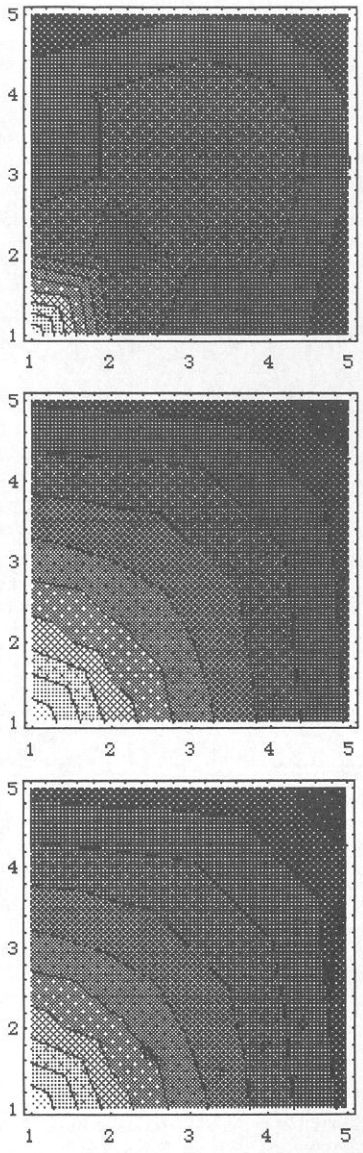

COMPLEX BOUNDARY IMPEDANCE

(a)

MEDIUM FREQUENCY
Side = 0.5 Wavelength

(b)

LOW FREQUENCY
Side = 0.05 Wavelength

(c)

VERY LOW FREQUENCY
Side = 0.005 Wavelength

Fig. 12. Pressure contour distribution plots for the model of Fig. 10, for a boundary termination that is mass reactive at low frequencies, and absorptive at high frequencies. (a) Mid frequency where the side walls are 0.5 wavelength long. (b) Low frequency where the sidewalls are 0.05 wavelength long. (c) Very low frequency where the sidewalls are 0.005 wavelength long. Note that as the frequency is lowered, the pressure distribution always decreases with distance from the source, even at the lowest frequency.